Heliyon 10 (2024) e25070

Contents lists available at ScienceDirect

Heliyon

journal homepage: www.cell.com/heliyon

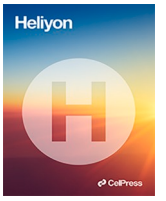

Research article

Thermal performance of Joule heating in radiative Eyring-Powell nanofluid with Arrhenius activation energy and gyrotactic motile microorganisms

Usman Ali [a,*], Muhammad Irfan [b]

[a] School of Mathematical Sciences, Zhejiang Normal University, 321004, Jinhua, China
[b] Department of Mathematical Sciences Federal Urdu University of Arts, Sciences & Technology, Islamabad, 44000, Pakistan

ARTICLE INFO

Keywords:
Eyring-Powell nanofluid
Bioconvection nanofluid
Arrhenius activation energy
Joule heating
New mass flux relation

ABSTRACT

Background: Bioconvection is the term for macroscopic convection of particles accompanied by a variable density gradient and a cluster of swimming microorganisms. The accumulation of gyrotactic microbes in the nanoparticles is important to exaggerate the thermal efficacy of various structures for instance, germs powered micro-churns, microbial fuel cubicles, micro-fluidics policies, and chip-designed micro plans like bio-microstructures.
Purpose: Here approach in the current effort is to present an innovative study of bio-convection owing to gyrotactic microbes in a nanofluid comprising non-uniform heat source/sink, space and temperature-dependent viscosity and Joule dissipation. The physical constraints such as convective-surface and new mass flux conditions are examined for *3D* Eyring-Powell magneto-radiative nanofluid via porous stretched sheet.
Method: ology: Over suitable similarity alterations, the related non-linear flow, temperature, and concentration phenomena, equations are altered into non-linear equations. By combining the shooting methodology with the Runge-Kutta fourth-order technique is applied to get numerical solutions. A thorough investigation for the impact of important non-dimensional thermophysical parameters regulating flow characteristics is carried out.
Motivation: Lots of the studies on nanofluids realize their performance therefore that they can be exploited where conventional heat transport development is paramount as in numerous engineering uses, micro-electronics, transportation in addition to foodstuff and bio-medicine. The gyrotactic microbes flow in nanofluids has attained great devotion amongst researchers and the scientist community because of its works in numerous areas of bio-technology. The benefits of counting nanoparticles in mobile microbe's deferral can be established in micro-scale involvement and stability of nanofluid.
Significant results: For a few chosen parameters, the computed results for friction factor and transport for motile microorganism values are shown. The computed numerical results for parameters of engineering interest are given using tables. Furthermore, the recent solutions are stable with the former stated results and excellent association is found. The temperature of the fluid exaggerates for higher values of thermo-Biot and radiation parameter; however, Peclet and bio-convective Lewis's factor decay the motile microorganisms' field of Eyring-Powell fluid. The concentration field also enhances the activation energy parameter.

* Corresponding author.
E-mail address: usmanali@zjnu.edu.cn (U. Ali).

https://doi.org/10.1016/j.heliyon.2024.e25070
Received 18 August 2023; Received in revised form 7 January 2024; Accepted 19 January 2024
Available online 20 January 2024

Nomenclature

(u, v, w)	Velocity components
u_w, v_w	Stretching velocity
a, b	Constant
T, T_∞	Surface temperature, Ambient temperature
C_∞, C	Ambient and Surface concentration
c_p	Specific heat at constant pressure
D_M	Mass diffusivity
p	Pressure
I	Identity tensor
A_1	First Rivlin Erickson tensor
K_r	Reaction rate constant
N	Microorganisms' concentration
M	Magnetic factor
Pr	Prandtl number
Rd	radiation factor
N_r	Buoyancy ratio parameter
Pr	Prandtl number
E	Activation energy
n	Fitted rate constant
k	Thermal conductivity (W/mK)
W_c	Velocity of gyrotactic cells
D_T, D_B	Thermophoresis and Brownian motion (m^2/s)
$B_\circ$	Magnetic field coefficient
g	Gravitational acceleration (m/s^2)
q_r	radiative heat flux, (W/s^2)
k^*	Absorption coefficient $(1/m)$
Nt, Nb	Thermophoresis and Brownian factors
Le	Lewis factor
Lb	Bioconvection Lewis factor

Greek letters

θ	Dimensionless temperature
φ	Dimensionless concentration
μ	Apparent viscosity
ρ_f	Density of fluid
α	Velocity slip parameter
κ	Boltzmann constant
$\gamma_\circ$	Velocity slip
β_C, β_T	Solutal and thermo expansion factors
ν	Kinematic viscosity
α_1	Thermal Diffusivity
σ_1	Chemical reaction parameter
Re_x	Local Reynolds number
δ	Temperature difference parameter
σ	Electrical conductivity
σ^*	Stefan-Boltzman constant
λ	Mixed convection parameter
ψ	Stream function
ζ	Similarity variable

1. Introduction

In reality, Bio-convection is the creation of forms in the deferrals of micro-organisms, for instance, algae and microbes. The association offers properties for micro-organisms to swim self-possessed. Due to the self-leaning microbes in the stated form, the fluid features can be reformed. Furthermore, Bio-convection is a natural progression that arises as microorganisms transport accidently in single-celled or colony-like formation. The guiding motion of numerous systems of micro-organisms is the base for several bio-convection structures. Significance of bioconvection can be comprehended in a diversity of bio-microsystems, for instance bio-

technology associated to enzyme bio-sensors, mass moving and fraternization [1,2]. Kuznetsov investigated that the existences of nano-particles also decrease/increase the critical Rayleigh number, which depends on whether the elementary nano-particle distribution is dense in top or in bottom. The bioconvective flow relevant to nanoliquid in free stream fluctuating space was explained by B'eg et al. [3]. Their study examined the stronger impact of bioconvection factor on the heat and motile micro-organism numbers. In the light of improved heat flux theories, Nagendramma et al. [4] investigated narrowing shallow flow of Casson nanofluid including micro-organisms. This study mentions that the velocity distribution is larger and positive for values of the Casson parameter compared with when it is infinite or negative. Moreover, opposite phenomena occurred for temperature-concentration fields. Elogail et al. [5] detailed the characterization of oxytactic microorganisms and documented the blood-vessels circulation of nanoparticles. The bioconvection characteristics of Prandtl nanofluid across permeable surfaces were established by Mekheimer and Ramadan [6].

Their outcomes show the higher motile microorganism's field for the case of shrinking sheet in comparison with stretching sheet. Moreover, the temperature and velocity fields enhanced in the absence of microorganisms and nanoparticles. The effect of dependent viscosity features on bioconvective flow for Casson-nanoliquid over an accelerating surface was discussed by Khaled and Khan [7]. The radiation and heating source factors enhanced the temperature profile; however, occurrence of Eyring Powell parameter and activation energy develops the nano-materials concentration field. Additional related prose have explored in Refs. [8–16].

Due to its impact on the features of heat transport on the surface, the exploration of temperature of the convective-surface under physical constraints [17–22] attracted interest. Many researchers looked at convective heat transfer analysis because of its vital usages such as thermal energy storage, nuclear power plants, and steam turbines. The nanofluid study under a uniform shear stress exerted due to surface-temperature convection limitations past an expanding or contracting surface was studied by Yacob et al. [23]. In the mixed convective radiative stream of the Maxwell nanofluid, Husian et al. [24] investigated twofold stratified and magnetized flux perception. Zaidi and Mohyud-Din [25] discussed impact of Joule heating in MHD liquid through wall in the case of convective temperature scenario and a Darcy Forchheimer expanded model. Islam et al. [26] investigation of non-Newtonian Casson liquid gesticulation with motile micro-organisms past an elongated surface taken into account over an extended Darcy Forchheimer model. The motile density profile showed the declining performance for the larger values of Lewis and bioconvection Peclet numbers in their work. Additionally, there is an improvement in the skin friction coefficient and Nusselt number for rise in the magnetic and nonlinear radiation factors. According to Shoaib et al. [27] impact of heat radiation on hybrid nanofluid flow with carbon nanoparticles across an elongating sheet is examined. They reported that the accuracy level of relative errors is up to 1e-15, establishing the value and consistency of the computational method. Also, observed that an increase in magnetic effect, rotation parameter, Biot number the transfer rate of heat enhanced.

In many residential, industrial, engineering, and commercial establishments, heat transfer is a crucial activity. To keep things running smoothly at each of these sites, heat must be added, taken out, or transmitted from one operation to another efficiently and effectively. Additionally, a variety of factors contribute to heat transfer. This could include internal heat creation and absorption, viscous dissipation (frictional heat), and non-uniform heat sources and sinks. In order to analyze the aforementioned characteristics of heat transport, this study included all relevant components in the energy equation. By including the radiation effect, the heat transport work on viscous fluid to a stretched surface increases a novel characteristic. Numerous important uses of these radiative effects exist in industrial and the physical disciplines. These effects are especially helpful in intense thermal processing and space-technology. In heat transfer analysis, however, a temperature and spatially dependent heat source or sink is crucial, and such effects have been documented by numerous authors in a variety of geometries. The concerned literature can be found in Refs. [28–34].

Recently the scientific works suggests that the thermophysical features in a Powell-Eyring nanofluid over a stretched sheet in contrast with bioconvection motile organisms are rarely conferred. Nanofluid has a great importance in many real-world applications. Firstly, the originality of modern work is based on the presence of nanoflulid because nanofluid is a smart liquid, where the transport of heat can be condensed or improved at will. The petroleum removal, chemical split-up progressions, enhancing of prosthetic nature controllers, plummeting friction in oil tubes, bio nano-fuel cells are some uses of nanofluid. Secondly, the presence of gyrotactic microbes in nanofluids has attained great consideration among the researchers and scientists because of its works in few regions of science and bio-technology. There is the prospect of exploiting microorganisms with nanofluids in several bio-microsystems, for instance, the optimization of fibers creation and to estimate harmfulness of nano-particles in chip-made micro-devices. Third, the fluid flow combined with activation energy and chemical reaction has well-known uses which comprise the damage of crops due to icing, paper developed, food dispensation, tiles, ventilation, and water mixtures. Lastly, the exploited process of shooting with RK fourth order solved highly nonlinear equations. Now, the limitation communicates to the base liquid's lesser ability for heat transference, which indicates to useless thermal diffusion. The essential dynamic force behind this effort is to comprise nanoparticles for heat transport and progress thermal conductivity. The innovative component of this work is the bioconvection of microorganisms, which avoids the potential settling of nano objects.

2. Mathematical conceptualization

This segment describes the three-dimensional Eyring-Powell flow on a bi-directionally stretched surface where the fluid assumes to be upon $z > 0$. The surface considered to be elongated in the longitude-direction along velocity $(u_w(x) = a\,x)$, also transverse direction with $v_w(y) = by$, where a, b denotes degrees of stretch. The components for velocity that is $(u, v$ and $w)$ each is reached in the $(x, y$ and z- directions) see Fig. 1. The mathematical model for Powell-Eyring fluid exploits the influence of nanoparticles, concentration of nanoparticles and microorganisms reported as follows. Further, the Cauchy stress tensor $(\widehat{\tau})$ for Powell-Eying fluid model is defined in Eqs. (1)–(3):

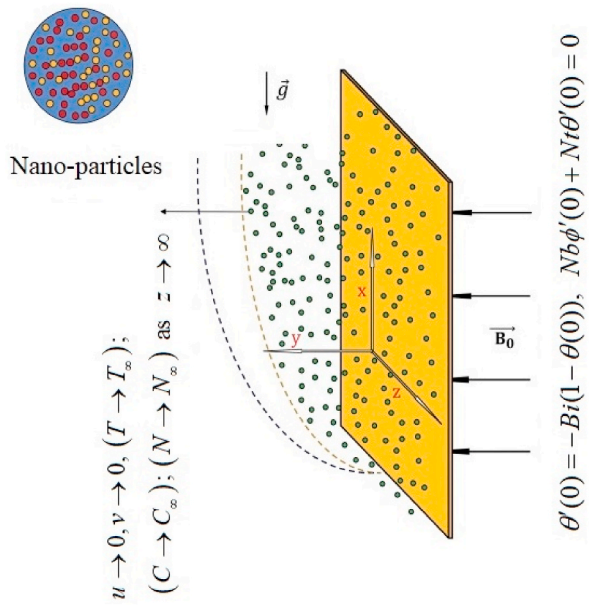

Fig. [1]. Physical illustration of the problem.

$$\hat{\tau} = \tau - Ip, \tag{1}$$

$$\rho_f a_i = \sigma(J \times B) + \nabla.(\tau_{ij}) - \nabla p, \tag{2}$$

Here, p as pressure, I be the identity-tensor, σ is fluid's electrical-conductivity, $\tau_{i\,j}$ as extra stress tensor for the Powell-Eyring model and expressed as

$$\tau_{i\,j} = \mu\left(\frac{\partial u_i}{\partial x_j}\right) + \left(\frac{1}{\beta_1}\right)\sinh^{-1}\left[\frac{1}{c^*}\left(\frac{\partial u_i}{\partial x_j}\right)\right], \tag{3}$$

where, μ as coefficient of viscosity, β_1, c^* are characteristics of Powell - Eyring fluid as given in equation [4],

$$\sinh^{-1}\left[\frac{1}{c^*}\left(\frac{\partial u_i}{\partial x_j}\right)\right] \cong -\frac{1}{6}\left(\frac{1}{c^*}\frac{\partial u_i}{\partial x_j}\right)^3 + \frac{1}{c^*}\left(\frac{\partial u_i}{\partial x_j}\right), \text{ where } \left|\frac{\partial u_i}{\partial x_j}\frac{1}{c^*}\right| < 1, \tag{4}$$

Now, by implying these principles, the equation of conservation of mass, momentum, energy and bioconvection motile microorganisms are defined [7,8] as follows Eqs. (5)–(10):

$$\frac{\partial w}{\partial z} + \frac{\partial v}{\partial y} + \frac{\partial u}{\partial x} = 0, \tag{5}$$

$$\begin{aligned} w\frac{\partial v}{\partial z} + v\frac{\partial v}{\partial y} + u\frac{\partial v}{\partial x} = &\left(\frac{1}{\rho_f \beta_1 c^*} + \upsilon\right)\frac{\partial^2 u}{\partial z^2} - \frac{1}{2\rho_f \beta_1 c^{*3}}\left(\frac{\partial u}{\partial z}\right)^2\frac{\partial^2 u}{\partial z^2} - \left(\frac{\sigma B_\circ^2}{\rho_f} + \frac{\upsilon k_2}{K^*}\right)u \\ &+\frac{1}{\rho_f}\left[\begin{matrix}(1-C_f)(T-T_\infty)\rho_f \beta^{**} g - (C-C_\infty)(\rho_p - \rho_f)g \\ -(N-N_\infty)\,(\rho_m - \rho_f)g\gamma^*\end{matrix}\right], \end{aligned} \tag{6}$$

$$w\frac{\partial v}{\partial z} + v\frac{\partial v}{\partial y} + u\frac{\partial v}{\partial x} = \left(\upsilon + \frac{1}{\rho_f \beta_1 c^*}\right)\frac{\partial^2 v}{\partial z^2} - \frac{1}{2\rho_f \beta_1 c^{*3}}\left(\frac{\partial v}{\partial z}\right)^2\frac{\partial^2 v}{\partial z^2} - \left(\frac{\sigma B_\circ^2}{\rho_f} + \frac{\upsilon k_2}{K^*}\right)v, \tag{7}$$

$$\begin{aligned} w\frac{\partial T}{\partial z} + v\frac{\partial T}{\partial y} + u\frac{\partial T}{\partial x} = &\left(\alpha^* + \frac{16\sigma^* T_\infty^3}{3k^*(\rho c)_p}\right)\frac{\partial^2 T}{\partial z^2} + \tau\left[D_B\frac{\partial C}{\partial z}\frac{\partial T}{\partial z} + \frac{D_T}{T_\infty}\left(\frac{\partial T}{\partial z}\right)^2\right] + \frac{q'''}{(\rho c)_p} \\ &+\frac{\sigma B_\circ^2}{(\rho c)_p}(u^2 + v^2) + \frac{\mu}{(\rho c)_p}\left[\left(\frac{\partial v}{\partial z}\right)^2 + \left(\frac{\partial u}{\partial z}\right)^2\right], \end{aligned} \tag{8}$$

$$w\frac{\partial C}{\partial z} + v\frac{\partial C}{\partial y} + u\frac{\partial C}{\partial x} = \frac{D_T}{T_\infty}\left(\frac{\partial^2 T}{\partial z^2}\right) + D_B\left(\frac{\partial^2 C}{\partial z^2}\right) - K_r^2\left(\frac{T}{T_\infty}\right)^n (C - C_\infty)\exp\left(\frac{-E_a}{\kappa T}\right), \tag{9}$$

$$u\frac{\partial N}{\partial x}+v\frac{\partial N}{\partial y}+w\frac{\partial N}{\partial z}+\frac{bW_c}{\Delta C}\left[\frac{\partial}{\partial z}\left(N\frac{\partial C}{\partial z}\right)\right]=D_m\left(\frac{\partial^2 N}{\partial z^2}\right), \tag{10}$$

The physical constraints for the flow model are utilized as reported in Eqs (11) and (12),

$$\left(u=\gamma_*\frac{\partial u}{\partial z}+u_w(x)\right);\ \left(v=\gamma_*\frac{\partial v}{\partial z}+v_w(y)\right);\ (w=0),\ -k\frac{\partial T}{\partial z}=h_f\left(T_f-T\right), D_B\frac{\partial C}{\partial z}+\frac{\partial T}{\partial z}\frac{D_T}{T_\infty}=0, N=N_w, \tag{11}$$

$$u\to 0, v\to 0, (T\to T_\infty);\quad (C\to C_\infty);\ \ (N\to N_\infty)\ \text{as}\quad z\to\infty \tag{12}$$

where, ν as kinematic viscosity, ρ_p as nanoparticle density, ρ_f fluid density, the gravity g, and magnetic field strength B_*, β^{**} as coefficient of volume suspension. Further, the nanoparticle temperature is termed as T, $\alpha^*=\frac{k}{(\rho c)_f}$, $\tau=\frac{(\rho c)_p}{(\rho c)_f}$ are the thermal diffusivity and heat capacity ration, c as volume fraction constant, K^* permeability of porous media, k_2 porous media, σ^* Stefan-Boltzmann constant, k^* is the average absorption constant, k thermal conductivity, D_B, D_T are the Brownian motion constant and coefficient of thermophoretic diffusion, K_r the chemical reaction constant, the activation energy constant E_a, $n(-1<n<1)$ is the fitted rate constant, N the microorganism's concentration, W_c is velocity of gyrotactic cells, γ_* a slip constant, and h_f a high frequency heat transmission coefficient. Additionally, $q'''=\frac{ku_w(x)}{x\upsilon}[A_1(T_f-T_\infty)f'+B_1(T-T_\infty)]$ as non-uniform heat sink/source and $K_r\left(\frac{T}{T_\infty}\right)^m exp\left(-\frac{E_a}{\kappa T}\right)$ named as Arrhenius equation in modified form, $\kappa=8.61\times 10^5 eV/K$ as Boltzmann constant.

2.1. Suitable transformations

The similarity transformations in eq (13) are:

$$\zeta=\sqrt{\frac{a}{\upsilon}}z^2, u=axf'(\zeta), v=byg'(\zeta), w=-\sqrt{a\nu}[f(\zeta)+g(\zeta)], \theta(\zeta)=\frac{T-T_\infty}{T_f-T_\infty}, \varphi(\zeta)=\frac{C-C_\infty}{C_\infty}, \chi(\zeta)=\frac{N-N_\infty}{N_w-N_\infty}, \tag{13}$$

Using the above transformation, we have the followings ODEs i.e., Eqs. (14)–(20)

$$(1+G)f'''-f'^2-(s_1G)f''^2f'''+f''(g+f)-Mf'+\lambda(\theta-N_r\varphi-R_b\chi)=0, \tag{14}$$

$$(1+G)g'''-(g')^2+g''(f+g)-Gs_2(g'')^2g'''-g'M=0, \tag{15}$$

$$\left(1+\frac{4}{3}Rd\right)\theta''+\Pr\left[\theta'(f+g)+Nt(\theta')^2+Nb\theta'\varphi'\right]+\Pr(A_1f'+B_1\theta)+Ec_x\Pr\left[(f'')^2+M(f')^2\right] +Ec_y\Pr\left[(g'')^2+M(g')^2\right]=0, \tag{16}$$

$$\varphi''+\Pr Le(f+g)\varphi'+\frac{Nt}{Nb}\theta''-\Pr Le\sigma_1(1+\delta\theta)^n\exp\left(\frac{-E}{1+\delta\theta}\right)\varphi=0, \tag{17}$$

$$\chi''+Lbf\chi'-\mathrm{Pe}[\varphi''(\chi+\Omega)+\chi'\varphi']=0, \tag{18}$$

The relevant physical constraints are as follows.

$$\begin{aligned} &f(0)=0, g(0)=0;\ \ (f'(0)=1+\alpha f''(0));\ \ g'(0)=\beta+\alpha g''(0),\\ &\theta'(0)=-Bi(1-\theta(0)), Nb\varphi'(0)+Nt\theta'(0)=0, \chi(0)=1, \end{aligned} \tag{19}$$

$$f'(\infty)\to 0, g'(\infty)\to 0, \theta(\infty)\to 0, \varphi(\infty)\to 0, \chi'(\infty)\to 0, \tag{20}$$

It should be noted that the above expressions are locally similar. Thus, physical quantity (dimensionless) in Eq. (14)–(18) subject to physical constraints given in Eq. (19) and (20) are defined as non-Newtonian parameters $((G, s_1, s_2))$, magnetic parameter M, mixed convection parameter λ, constant buoyancy coefficient N_r, bio-convection Rayleigh number R_b, radiation parameter Rd, The Eckert number along x and y-direction are Ec_x and Ec_y, parameter of Brownian motion Nb, parameter of thermophoretic Nt, Prandtl number Pr, Lb bio-convective Lewis number, energy-activation parameter E; Lewis number Le, chemical reaction parameter σ_1, temperature difference parameter δ, Peclet number Pe, the constant of microorganisms concentration difference Ω, velocity slip parameter α, stretching ratio parameter β and Biot number Bi. Also, A_1 and B_1 shows the dependence on space and temperature parameter or $A_1>0, B_1>0$ means heat source case and $A_1<0, B_1<0$ means sink case, which is formulated mathematically in Eq (21).

$$G=\frac{1}{\mu\beta_1 c^*}, s_1=\frac{a^3x^2}{2c^{*2}\nu}, s_2=\frac{b^3y^2}{2c^{*2}\nu}, M=\frac{\sigma^* B_*^2}{a\rho_f}+\frac{\nu k_2}{aK^*}, \beta=\frac{b}{a}, \lambda=\frac{\beta^{**}\gamma^*(1-C_\infty)(T_f-T_\infty)}{au_w},$$
$$N_r=\frac{(\rho_p-\rho_f)C_\infty}{\rho_f(C-C_\infty)T_\infty\beta^{**}}, R_b=\frac{\gamma^*(\rho_m-\rho_f)(n_w-n_\infty)g}{\beta^{**}\rho_f(C-C_\infty)T_\infty}, Rd=\frac{4\sigma^*T_\infty^3}{k^*k}, Ec_x=\frac{u_w^2}{c_p(T_f-T_\infty)}$$
$$Ec_y=\frac{-v_w^2}{c_p(-T_\infty+T_f)}, Nb=\frac{\tau D_B(C_\infty)}{\nu}, Nt=\frac{\tau D_T(T_w-T_\infty)}{T_\infty\nu}, \mathrm{Pe}=\frac{aW_c}{D_m}, \mathrm{Pr}=\frac{\nu}{\alpha^*}, Le=\frac{\alpha^*}{D_B},$$
$$\sigma_1=\frac{K_r^2}{a}, \delta=\frac{-T_\infty+T_w}{T_\infty}, E=\frac{E_a}{\kappa T_\infty}, Lb=\frac{\nu}{D_m}, Bi=\frac{h_f}{k}\sqrt{\frac{\nu}{a}}, \Omega=\frac{N_\infty}{N_w-N_\infty}, \alpha=\gamma_*\left(\frac{\nu}{a}\right)^{-1/2}, \tag{21}$$

3. Physical quantities

The C_{f_x} and C_{f_y} are examined in Eqs (22) and (23),

$$C_{fx}=\frac{\tau_{wx}}{\rho_f u_u^2}, C_{fy}=\frac{\tau_{wy}}{\rho_f u_w^2}, \tau_{wx}=\mu\left(\frac{\partial u}{\partial z}\right)_{z=0}, \tau_{wy}=\mu\left(\frac{\partial v}{\partial z}\right)_{z=0}, \tag{22}$$

The thermal and motile transference past a surface to fluid produces mathematical relations as follows.

$$Nu_x=\frac{xq_w}{k(T_w-T_\infty)}, Nn_x=\frac{xq_n}{D_n(N_w-N_\infty)},$$
$$q_w=-k\left(\frac{\partial T}{\partial z}\right)_{z=0}-\left(\frac{16\sigma^*T_\infty^3}{3k^*(\rho c)_p}\right)_{z=0}, q_n=-D_n\left(\frac{\partial N}{\partial z}\right)_{z=0}, \tag{23}$$

where q_w, q_n are surface heat flux and motile microorganisms mass flux. Further, the non-dimensional form of Eq. (23) are given in equation (24),

$$C_{fx}\mathrm{Re}_x^{0.5}=-f''(0), C_{fy}\mathrm{Re}_y^{0.5}=-g''(0),$$
$$\frac{Nu_x}{\mathrm{Re}_x^{0.5}}=-(1+4Rd)\theta'(0), \frac{Nn_x}{\mathrm{Re}_x^{0.5}}=-\chi'(0), \tag{24}$$

4. Working Rule

Here the initial value problem have been attained via switching the BCs $(z_2(\infty), z_5(\infty), z_7(\infty), z_9(\infty), z_{11}(\infty))$, with the missing ICs $(z_3(0)=u_1, z_6(0)=u_2, z_8(0)=u_3, z_9(0)=u_4, z_{12}(0)=u_5)$. The attained Eqs., solved via R-K-F process considering $(z_3(0), z_6(0), z_8(0), z_9(0), z_{12}(0))$ as initial estimates. The convergence exists if $|z_i(\infty)-\widetilde{z}_i(\infty)|$ for $(i=2,5,7,9,11)$, and computed values of $\widetilde{z}_i(\infty)$ are lesser than 0.000001 or tolerance faults. Furthermore, Newton's method helps if the considered outcomes doesn't fulfill the conditions until the convergence achieved.

3.1. Procedure

Pursuing the obligatory procedure, the set of Eq. (14)–(20) are first transmuted into first order ODE's (25)–(33) by following way:

$$f(\zeta)=z_1, f'(\zeta)=z_2, f''(\zeta)=z_3, f'''(\zeta)=z_3', (g=z_4), g'(\zeta)=z_5; \quad (g''(\zeta)=z_6); \quad \left(g'''(\zeta)=z_6'\right), \tag{25}$$

$$\theta=z_7; \quad (\theta'(\zeta)=z_8), \left(\theta''(\zeta)=z_8'\right); \ (\varphi=z_9); \ \varphi'(\zeta)=z_{10}, \varphi''(\zeta)=z_{10}', \tag{26}$$

$$\chi(\zeta)=z_{11}, \chi'(\zeta)=z_{12}, \chi''(\zeta)=z_{12}', \tag{27}$$

$$z_1'=z_2,$$
$$z_2'=z_3,$$
$$z_3'=\frac{\left[(z_2)^2-(z_1+z_4)z_3+Mz_2-\lambda(z_7-Nrz_9-Rbz_{11})\right]}{(1+G-Gs_1z_3^2)},$$
$$z_4'=z_5,$$
$$z_5'=z_6,$$
$$z_6'=\frac{\left[(z_5)^2-(z_1+z_4)z_6+Gsz_6+Mz_5\right]}{(1+G-Gs_2z_6^2)}, \tag{28}$$

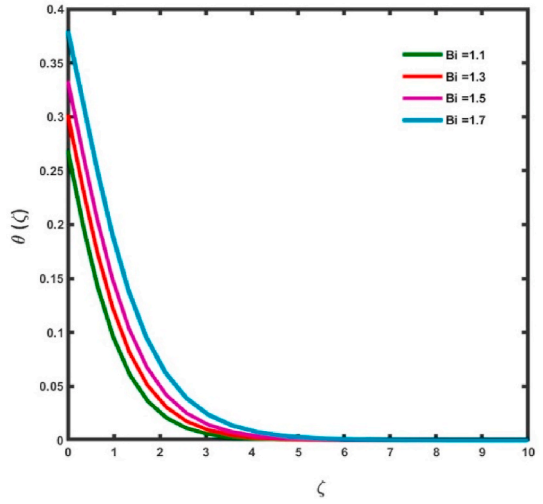

Fig. (2). Impacts for Bi upon $\theta(\zeta)$.

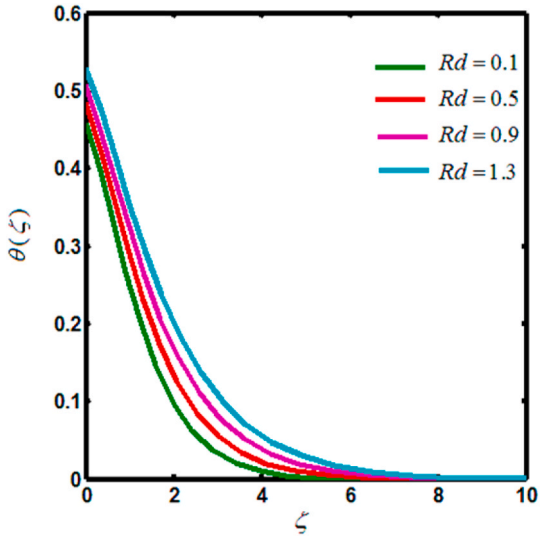

Fig. (3). Impacts for Rd upon $\theta(\zeta)$.

$$
\begin{aligned}
&z_7' = z_8,\\
&z_8' = \left(\frac{-3}{3+4Rd}\right)\begin{bmatrix}\Pr\left((z_1+z_4)z_8 + Nbz_8z_{10} + Ntz_8^2\right) + A_1z_2 + B_1z_7\\ +Ec_x\Pr\left(z_3^2 + Mz_2^2\right) + Ec_y\Pr\left(z_6^2 + Mz_5^2\right)\end{bmatrix},\\
&z_9' = z_{10},\\
&z_{10}' = -\left[\Pr Le(z_1+z_4)z_{10} + \left(\frac{Nt}{Nb}\right)z_8' - Le\Pr\left(\sigma(1+\delta z_7)^n\exp\left(\frac{-E}{1+\delta z_7}\right)\right)z_9\right],
\end{aligned}
\tag{29}
$$

$$
\begin{aligned}
&z_{10}' = z_{11},\\
&z_{11}' = z_{12},\\
&z_{12}' = -Lb(z_1z_{12}) + \mathrm{Pe}\left(z_{10}'(z_{11}+\Omega) + z_{10}z_{12}\right),
\end{aligned}
\tag{30}
$$

$$
z_1(0) = 0, z_2(0) = 1 + \alpha z_3(0), z_2(\infty) = 0, z_4(\zeta) = 0, z_5(\zeta) = \beta + \alpha z_6(0), z_5(\infty) = 0,
\tag{31}
$$

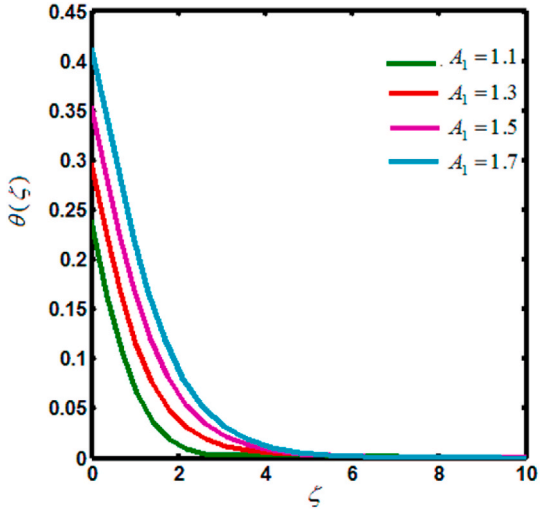

Fig. (4). Impacts for A_1 upon $\theta(\zeta)$.

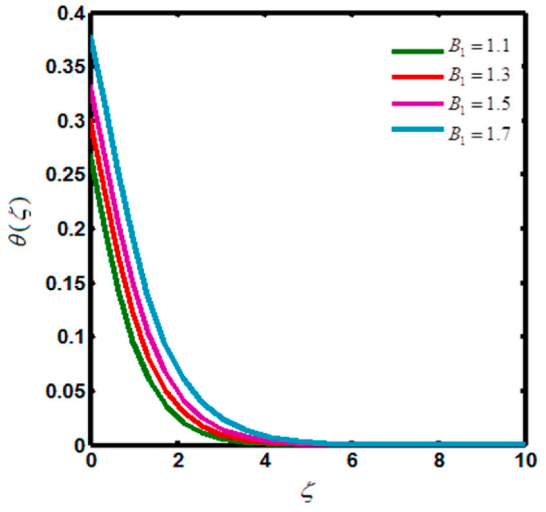

Fig. (5). Impacts for B_1 upon $\theta(\zeta)$.

$$z_7(0) = 1 + \frac{z_8(0)}{Bi}, z_7(\infty) = 0, z_{10}(0) = \frac{-Nt}{Nb} z_8(0), \tag{32}$$

$$z_{11}(0) = 1, z_{11}(\infty) = 0. \tag{33}$$

4. Results and discussion

The numerical solutions have been computed graphically and in tabular representations. These variables effect on temperature, concentration and motile microorganism's profiles as well as the transport rate of motile microorganisms.

4.1. Temperature profile

Figs. 2 and 3 explain the influence of the Biot number $Bi(= 1.1, 1.3, 1.5, 1.7)$ and radiation factor $Rd = 0.1, 0.3, 0.5, 0.7$ on the temperature profile. For fixed values, $M = \lambda = s_1 = s_2 = Nb = Nt = 0.1, \Pr = 2.5, \alpha = 0.5, A_1 = B_1 = Le = 0.5, \sigma_1 = \delta = 1.1, Lb = Pe = \Omega = 0.5$, these parameters report the enhancing behavior for higher estimations. Actually, growing the values of *Bi* increases the transportation of transport which increases the temperature field. Moreover, a constant temperature of temperature is attained for larger values of (*Bi*) which means that the heat transmission number goes in height. Hence, the enhancing trend is appeared for temperature. Furthermore, the similar behavior occur for *Rd* and enhance the temperate profile. Larger values of *Rd* made significant

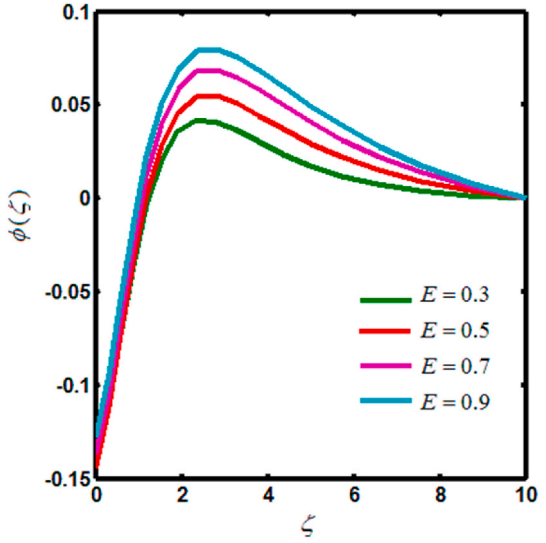

Fig (6). Impacts for E upon $\varphi(\zeta)$.

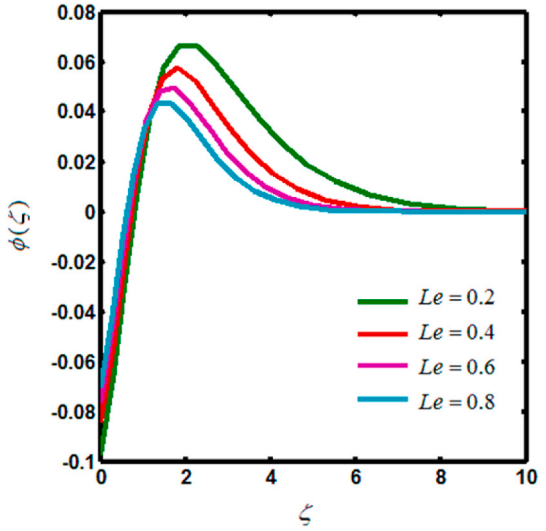

Fig (7). Impacts for Le upon $\varphi(\zeta)$.

heat during the process of radiation in working fluid which increase the temperature field.

Figs. 4 and 5 depicted for $A_1 > 0, B_1 > 0$ factors on the temperature profile. Here, $A_1 > 0, B_1 > 0$ show the enhancing trend for fixed values, $M = \lambda = s_1 = s_2 = Nb = Nt = 0.1, \Pr = 2.5, \alpha = 0.5, Rd = Bi = Le = 0.5, \sigma_1 = \delta = 1.1, Lb = Pe = \Omega = 0.5$ The parameters heat source be influenced by on space and temperature illustrates an energetic amount in enhancing of heat transfer. Thus, these arrangements spectacles that the temperature profile is increasing function $A_1 > 0, B_1 > 0$. Physically, the energy is created for the process of higher values of $A_1 > 0$ which enhance the temperature profile. Hence, an outcomes that similar behavior occur for both graphs Figures (4) and (5).

4.2. Concentration profile

To portray the graphical depiction of activation energy parameter $E = 0.3, 0.5, 0.7, 0.9$ and Lewis number $Le = 0.2, 0.4, 0.6, 0.8$ on concentration profile Figs. 6 and 7 are sketched for

$M = \lambda = Nb = Nt = 0.1, \Pr = 2.5, \alpha = 0.5, Rd = Bi = 0.5, \sigma_1 = \delta = 1.1, Lb = Pe = \Omega = 0.5$. The concentration profile growing for E and decay for Le. Physically, a rise in E reduces the modified Arrhenius function, which rises the amount of generative chemical reactions. Furthermore, the higher values of E, the chemical reaction level between the species upturns and therefore, an rise in the concentration is detected. Fig. 7 analyze the impact of Lewis number (Le) and showing opposite trend compared to E. The higher Le

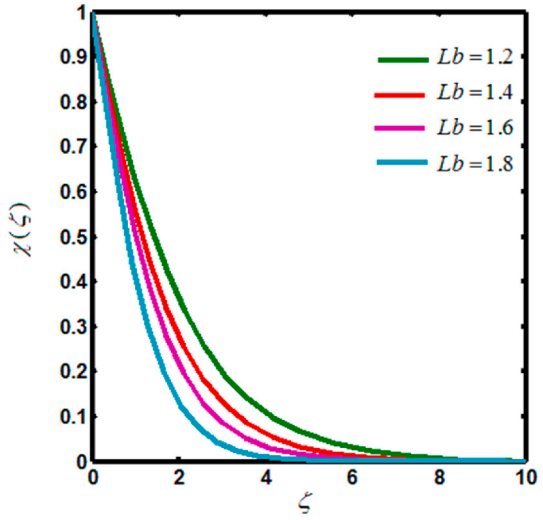

Fig (8). Impacts for *Lb* upon $\chi(\zeta)$.

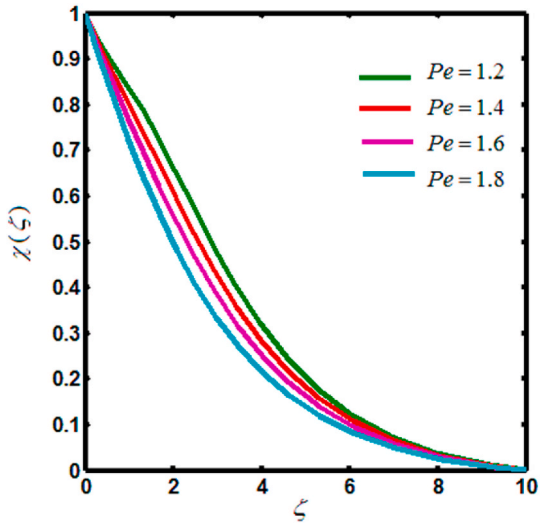

Fig (9). Impacts for *Pe* upon $\chi(\zeta)$.

signifies the relation influence of the thermal rate to species diffusion. *Le* has an inverse relation of diffusion coefficient and larger *Le* decays the diffusion coefficient which decays concentration profile.

4.3. Motile microorganisms profile

Figs. 8 and 9 explains the effect of bio-convective Lewis $Lb = 1.2, 1.4, 1.6, 1.8$ and bio-convective Peclet $Pe = 1.2, 1.4, 1.6, 1.8$ numbers, respectively on motile microorganism's profile. Taking, $M = 0.1, \lambda = Nb = Nt = 0.1, \mathrm{Pr} = 2.5, \alpha = 0.5, Rd = Bi = 0.5, \sigma_1 = \delta = 1.1, Le = E = \Omega = 0.5$. The decaying sketches have been noted for both *Pe* and *Lb* on χ. The physical aspect reports that the larger *Lb* is connected to less dispersion of motile microorganisms, so decaying behavior of curves is noted for χ. Fig. 9 explore the similar trend for higher values of *Pe*. When the values of *Pe* enhance the concentration of motile microorganisms decline.

4.4. Tabular results

Table 1 displays the numerical values of skin-friction coefficients for various values of magnetic parameter *M* when $\beta = 0.0, 0.5, 1.0$ and for β when $M = 0$ and 1.0. The corresponding values of skin-friction coefficient shows declining trend when *M* rises and $\beta = 0.5$. Also, $f''(0)$ and $g''(0)$ depicts an uplift for same values of *M* and β. When $\beta = 0$, the values of $g''(0)$ are zero, and thus, our problem is

Table 1
Table for skin friction against values of M while $\lambda = 0$.

M	β	$-f''(0)$ [23]	$-f''(0)$ Present	$-g''(0)$ [23]	$-g''(0)$ Present
0.0	0.0	1.00000	1.00000	0.0	0.0
1.0	–	1.414214	1.414213	0.0	0.0
0.0	0.5	1.093095	1.093095	0.465205	0.465205
1.0	–	1.476771	1.476770	0.679809	0.679809
0.0	1	1.173722	1.173722	1.173722	1.173722

Table 2
Table for Nusselt number for *Nb*, *Nt* and *Rd*.

Nb	*Nt*	*Rd*	$-\mathrm{Re}_x^{0.5}(1+4Rd)\theta'(0)$
2.0	2.0	0.2	0.9834
5.0			1.2864
10.0			2.7051
2.0	2.0		0.9834
	5.0		1.2243
	10.0		1.8193
	2.0	0.1	0.9154
		0.3	0.8294
		0.5	0.7867
		0.2	1.2489

Table 3
Table for $-\chi'(0)$ for various numeric of Pr, *Lb*, Ω and *Pe*.

Pr	*Lb*	Ω	*Pe*	$-\chi'(0)$
2.0	2.0	0.2	2.0	0.8723
5.0				1.1753
10.0				2.6960
2.0	2.0			0.8723
	5.0			1.2243
	10.0			1.8193
	2.0	0.1		0.9154
		0.3		0.8294
		0.5		0.7867
		0.2	0.1	1.2489
			1.0	1.1221
			2.0	0.8723

reduced to two-dimensional flow. When M grows, $f''(0)$ and $g''(0)$ rise in the same manner for $\beta = 1.0$. The transport of heat via larger values of *Nb*, *Nt* and *Rd* are explored in Table 2. The higher values of these factors *Nb*, *Nt* and *Rd* exaggerate the $-\mathrm{Re}_x^{0.5}(1+4Rd)\theta'(0)$. Table 3 presents the numerical values of $-\chi'(0)$ for Pr, *Lb*, Ω and *Pe*. This table analyze that the higher Pr and *Lb* enhanced the transport rate of motile microorganisms, whereas opposite behavior have been noted for Ω and *Pe*.

5. Conclusion

Here the concept of gyrotactic-swimming-microorganisms in magneto Eyring-Powell nanofluid have been explored. The influence of activation energy considering convective and new mass flux theory have been also examined. The keys facts of this study are.

- ➢ The temperature of Eyring-Powell fluid increased for radiation and Biot factor.
- ➢ The Lewis factor decayed the concentration profile; however, enhanced for *E*.
- ➢ Bio-convection Lewis (*Lb*) and Peclet number *Pe* declined the curves for motile microorganisms.
- ➢ The enhancing variation appears in the drag force against magnetic parameter *M*.
- ➢ The motile microorganism's transfer rate improved for greater Pr and *Lb*.

CRediT authorship contribution statement

Usman Ali: Writing – original draft, Methodology, Investigation, Data curation. **Muhammad Irfan:** Writing – review & editing, Writing – original draft, Software, Methodology, Formal analysis, Conceptualization.

Declaration of competing interest

The author declared no conflict of interest for this submission.

References

[1] A.V. Kuznetsov, The onset of nanofluid bioconvection in a suspension containing both nanoparticles and gyrotactic microorganisms, Int. Commun. Heat Mass Tran. 37 (2010) 1421–1425.
[2] A.V. Kuznetsov, Nanofluid bioconvection in water-based suspensions containing nanoparticles and oxytactic microorganisms: oscillatory instability, Nanoscale Res. Lett. 6 (2011) 1–13.
[3] O. Bég, M.J. Anwar, W.A. Khan, Bioconvective non-Newtonian nanofluid transport in porous media containing micro-organisms in a moving free stream, J. Mech. Med. Biol. 15 (2015) 1550071.
[4] V. Nagendramma, C.S.K. Raju, B. Mallikarjuna, S.A. Shehzad, A. Leelarathnam, 3D Casson nanofluid flow over slendering surface in a suspension of gyrotactic microorganisms with Cattaneo-Christov heat flux, Appl. Math. Mech. 5 (2018) 623–638.
[5] M.A. Elogail, K.S. Mekheimer, Modulated viscosity-dependent parameters for MHD blood flow in microvessels containing oxytactic microorganisms and nanoparticles, Symmetry 12 (2020) 2114.
[6] K.S. Mekheimer, S.F. Ramadan, New insight into gyrotactic microorganisms for bio-thermal convection of Prandtl nanofluid over a stretching/shrinking permeable sheet, SN Appl. Sci. 450 (2020) 1–11.
[7] K. Al-Khaledand, S.U. Khan, Thermal aspects of Casson nanoliquid with gyrotactic microorganisms, temperature-dependent viscosity, and variable thermal conductivity: bio-Technology and Thermal Applications, Inventions 5 (2020) 39.
[8] M. Khan, M. Irfan, W.A. Khan, Impact of nonlinear thermal radiation and gyrotactic microorganisms on the Magneto-Burgers nanofluid, Int. J. Mech. Sci. 130 (2017) 375–382, https://doi.org/10.1016/j.ijmecsci.2017.06.030.
[9] M. Muthtamilselvan, S. Suganya, Q.M. Al-Mdallal, Stagnation-point flow of the Williamson nanofluid containing gyrotactic micro-organisms, Proc. Natl. Acad. Sci., India, Sect. A 91 (2021) 633–648.
[10] W.A. Khan, N. Anjum, M. Waqas, S.Z. Abbas, M. Irfan, T. Muhammad, Impact of stratification phenomena on a nonlinear radiative flow of sutterby nanofluid, J. Mater. Res. Technol. 15 (2021) 306–314.
[11] Y.Q. Song, B.D. Obideyi, Nehad Ali Shah, I.L. Animasaun, Y.M. Mahrous, J.D. Chung, Significance of haphazard motion and thermal migration of alumina and copper nanoparticles across the dynamics of water and ethylene glycol on a convectively heated surface, Case Stud. Therm. Eng. 26 (2021) 101050.
[12] C. Wenhao, I.L. Animasaun, Yook Se-Jin, V.A. Oladipupo, X. Ji, Simulation of the dynamics of colloidal mixture of water with various nanoparticles at different levels of partial slip: ternary-hybrid nanofluid, Int. Commun. Heat Mass Tran. 135 (2022) 106069.
[13] S. Abdal, I. Siddique, D. Alrowaili, Q.M. Al-Mdallal, S. Hussain, Exploring the magnetohydrodynamic stretched flow of Williamson Maxwell nanofluid through porous matrix over a permeated sheet with bioconvection and activation energy, Sci. Rep. 278 (2022), https://doi.org/10.1038/s41598-021-04581-1.
[14] W.A. Khan, A. Ahmad, N. Anjum, S.Z. Abbas, W. Chammam, A. Riahi, H. Rebei, M. Zaway, Impact of nanoparticles and radiation phenomenon on viscoelastic fluid, Int. J. Mod. Phys. B 36 (2022) 2250049.
[15] R. Fathollahi, A. Alizadeh, Y. Safari, H. Nabi, M. Shamsborhan, F. Taghinia, Examination of bio convection with nanoparticles containing microorganisms under the influence of magnetism fields on vertical sheets by five-order Runge-Kutta method, Heliyon 9 (2023) e15982.
[16] S. Saranya, Q.M. Al-Mdallal, I.L. Animasaun, Shifted legendre collocation analysis of time-dependent Casson fluids and carreau fluids conveying tiny particles and gyrotactic microorganisms: dynamics on static and moving surfaces, Arabian J. Sci. Eng. 48 (2023) 3133–3155.
[17] A. Aziz, A similarity solution for laminar thermal boundary layer over a flat plate with a convective surface boundary condition, Commun. Nonlinear Sci. Numer. Simulat. 14 (2009) 1064–1068.
[18] M. Khan, M. Irfan, W.A. Khan, Heat transfer enhancement for Maxwell nanofluid flow subject to convective heat transport, Pramana - J. Phys. 92 (2019) 1–9.
[19] W.A. Khan, H. Sun, M. Shahzad, M. Ali, F. Sultan, M. Irfan, Importance of heat generation in chemically reactive flow subjected to convectively heated surface, Indian J. Phys. 95 (2021) 89–97.
[20] M. Nasir, M. Waqas, O. Anwar Bég, N. Zamri, H.J. Leonard, K. Guedri, Dynamics of tangent-hyperbolic nanoliquids configured by stratified extending surface: effects of transpiration, Robin conditions and dual stratifications, Int. Commun. Heat Mass Tran. 139 (2022) 106372.
[21] U. Ali, M. Irfan, Thermal aspects of multiple slip and Joule heating in a Casson fluid with viscous dissipation and thermo-sloutal convective conditions, Int. J. Mod. Phys. B 37 (2023) 2350043.
[22] S.K. Rawat, M. Yaseen, A. Shafiq, M. Kumar, Q.M. Al-Mdallal, Nanoparticle aggregation effect on nonlinear convective nanofluid flow over a stretched surface with linear and exponential heat source/sink, Int. J. Thermofluids 19 (2023) 100355.
[23] N.A. Yacob, A. Ishak, I. Pop, K. Vajravelu, Boundary layer flow past a stretching/shrinking surface beneath an external uniform shear flow with a convective surface boundary condition in a nanofluid, Nanoscale Res. Lett. 6 (2011) 1–7.
[24] T. Hussain, S. Hussain, T. Hayat, Impact of double stratification and magnetic field in mixed convective radiative flow of Maxwell nanofluid, J. Mol. Liquids 220 (2016) 870–878.
[25] Z.A. Zaidi, S.T. Mohyud-Din, Effect of joule heating and MHD in the presence of convective boundary condition for upper convected Maxwell fluid through wall jet, J. Mol. Liquids 230 (2017) 230–234.
[26] S. Islam, M. Jawad, A. Saeed, M. Zubair, A. Khan, S.S. Ahmad, Z. Shah, H. Alrabaiah, MHD Darcy-Forchheimer flow due to gyrotactic microorganisms of Casson nanoparticles over a stretched surface with convective boundary conditions, Phys. Scripta 96 (2020) 015206.
[27] M. Shoaib, M.A.Z. Raja, M.T. Sabir, S. Islam, Z. Shah, P. Kumam, H. Alrabaiah, Numerical investigation for rotating flow of MHD hybrid nanofluid with thermal radiation over a stretching sheet, Sci. Rep. 10 (2020) 1–15.
[28] U. Ali, K.U. Rehman, M.Y. Malik, I. Zehra, Thermal aspects of Carreau fluid around a wedge, Case Studies Ther. Eng. 12 (2018) 462–469.
[29] U. Ali, K.U. Rehman, M.Y. Malik, I. Zehra, Thermal and concentration aspects in Carreau viscosity model via wedge, Case Studies Ther. Eng. 12 (2018) 126–133.
[30] W.A. Khan, M. Waqas, W. Chammam, Z. Asghar, U.A. Nisar, S.Z. Abbas, Evaluating the characteristics of magnetic dipole for shear-thinning Williamson nanofluid with thermal radiation, Comput. Methods Prog. Biomedicine 191 (2020) 105396.
[31] M.S. Anwar, M. Irfan, M. Hussain, T. Muhammad, Z. Hussain, Heat Transfer in a Fractional Nanofluid Flow through Permeable Medium, Mathematical Problems Eng., 2022, https://doi.org/10.1155/2022/3390478.
[32] M. Irfan, Energy Transport Phenomenon via Joule Heating and Aspects of Arrhenius Activation Energy in Maxwell Nanofluid, Waves Random Complex Media, 2023, https://doi.org/10.1080/17455030.2023.2196348.
[33] I. Waini, S. Alabdulhady, A. Ishak, I. Pop, Viscous dissipation effects on hybrid nanofluid flow over a non-linearly shrinking sheet with power-law velocity, Heliyon 9 (2023) e20910.
[34] T. Hayat, S.A. Shehzad, M. Qasim, S. Asghar, Three-dimensional stretched flow via convective boundary condition and heat generation/absorption, Int. J. Numerical Methods Heat Fluid Flow 2 (2014) 342–358.